J. Phys. B: At. Mol. Opt. Phys. **33** (2000) 4939–4956. Printed in the UK PII: S0953-4075(00)16280-7

Circular dichroism in differential and integrated cross sections of free–free transitions in high-energy electron–atom scattering

Aurelia Cionga†, Fritz Ehlotzky‡ and Gabriela Zloh†

† Institute for Space Science, PO Box MG-23, R-76900 Bucharest, Romania
‡ Institute for Theoretical Physics, University of Innsbruck, Technikerstrasse 25, A-6020 Innsbruck, Austria

Received 11 August 2000

Abstract. In this paper high-energy electron scattering by hydrogen atoms in the presence of a laser field of moderate power and higher frequencies will be considered. For a superposition of a linearly and a circularly polarized laser beam we shall show that circular dichroism in the angular distribution can be predicted for the nonlinear two-photon transitions, if the dressing of the atomic target by the laser field is treated in second order of perturbation theory in which the coupling between the atomic bound and continuum states plays an essential role. Of special interest is that for particular configurations circular dichroism can be encountered not only in the differential but also in the integrated cross sections. To the best of our knowledge this is the first example of this kind and therefore this effect should become more easily accessible to observation.

1. Introduction

In the course of his experimental investigations on dispersion in liquids and gases, Cotton [1] detected circular dichroism. Since then dichroism has become a well known concept in classical optics. It denotes the property of certain materials to have absorption coefficients that depend on the state of polarization of the incident radiation field [2, 3]. This general notion was taken over into the investigation of problems of atomic or molecular interactions with a laser field. Of particular interest became the concept of circular dichroism in an angular distribution (CDAD). It refers to the differences between the fluxes of scattered or ionized electrons measured at definite spatial directions, caused by *left* and *right* circularly polarized (CP) laser light [4]. CDAD was found, for example, in the photoionization of polarized atoms and of oriented molecules [5]. In our present work we shall use the definition of CDAD that was introduced by Manakov *et al* [6], namely as the angular dependence of the difference between the differential cross sections (DCS) evaluated for the two helicities of the laser photons. In particular, we shall denote by CD the special case in which the angular integration of the differences between the left and right CP signals yields a non-vanishing result. In recent years, in the investigation of several other processes stimulated by laser fields, increasing care has been devoted to the effects caused by the different states of polarization of such fields. For example, the double photoionization of helium [7], x-ray scattering by unoriented systems [8, 9], electron impact excitation of autoionizing states of atoms excited by CP lasers [10] and several multiphoton processes [11–19] were investigated along these lines.

0953-4075/00/214939+18$30.00

In the following we want to consider the effect of the photon helicity in laser-induced and inverse bremsstrahlung for high-energy scattering of electrons by hydrogen atoms. In previous work [6, 12, 18] it was shown that for high-energy electron scattering CDAD cannot be encountered in the presence of CP laser light since it is a well known fact that in the first-order Born approximation we are always led to real scattering amplitudes. As was shown, however, by Manakov *et al* [6], CDAD can be predicted in laser-assisted potential scattering of electrons of low energy, provided the CP field has low frequency and low intensity and if the scattering amplitude becomes evaluated to higher orders in the Born series. On the other hand, in our present work we shall demonstrate that it is also possible to find CDAD effects for high scattering energies of the electrons if the *dressing of the atomic target* by the laser field is taken into account. In particular, we shall consider higher optical frequencies of the laser field and restrict ourselves to the use of moderate field intensities. In this case we can employ a hybrid-like treatment of the problem [20]. By this we mean that the interaction between the scattered electron and the laser field will be described by Gordon–Volkov solutions, while the laser-dressing of the atom can be evaluated within the framework of time-dependent perturbation theory (TDPT). Using this approximation, we can demonstrate that CDAD becomes a non-vanishing effect under the following conditions:

(a) the electromagnetic field is taken as a superposition of a linearly polarized (LP) and a circularly polarized field not necessarily propagating in the same direction;
(b) second-order TDPT is used to describe the dressing of the atomic electron by the two fields. Moreover,
(c) it is necessary to analyse the role of the virtual transitions between the bound and continuum states and to show that these transitions are essential in order to be able to predict the existence of CDAD effects. Of particular interest is the fact that, for certain scattering configurations, a helicity-dependent signal even persists after the cross sections were integrated over the azimuthal plane. It appears that our problem is the first example where such an effect could be observed.

The main part of the theory will be presented in section 2. In section 3 we shall consider the scattering matrix elements for two-photon transitions in the weak-field limit. In this limit a detailed numerical analysis of the angular dependence of the DCS on the helicity of the CP field in the case of the emission or absorption of two laser photons by the colliding system will follow in section 4 where we shall discuss two particularly interesting scattering configurations. The final section will be devoted to a summary of our findings and to a number of more general concluding remarks relevant to our process. We shall use atomic units (au) throughout this paper.

2. Basic equations

We consider free–free transitions in electron–hydrogen scattering in the presence of an electromagnetic field that is composed of a superposition of two laser beams. One beam is LP, with polarization vector $\vec{e}$, while the other one is CP with polarization vector $\vec{\varepsilon}$. The two beams will be permitted to propagate in different directions. For the sake of simplicity, we discuss here the case in which the two laser beams have the same frequency ω and intensity I. For optical frequencies we can employ the dipole approximation in which case the resulting

electric field can be described by

$$\vec{\mathcal{E}}(t) = \mathrm{i}\frac{\mathcal{E}_0}{2}\,(\vec{e} + \vec{\varepsilon})\exp(-\mathrm{i}\omega t) + \text{c.c.} \tag{1}$$

where the intensity of the laser field is given by $I = \mathcal{E}_0^2$.

Within the dipole approximation we could argue that this superposition can be described by a vector of elliptic polarization

$$\vec{\epsilon} = \frac{1}{\sqrt{2\left[1 + \mathrm{Re}(\vec{e}\cdot\vec{\varepsilon})\right]}}\,(\vec{e} + \vec{\varepsilon}) \tag{2}$$

since the directions of propagation of the two beams do not enter into the expression of the field (1). However, we are particularly interested to know whether the DCS will be sensitive to the helicity of the CP photons which is defined by

$$\xi = \mathrm{i}\vec{n}\cdot\left(\vec{\varepsilon}\times\vec{\varepsilon}^{\,*}\right). \tag{3}$$

This expression depends explicitly on the direction $\vec{n}$ of propagation of the CP laser beam. We therefore consider it necessary to present the analytic formalism for the above superposition of two laser fields. Moreover, this superposition of radiation fields permits an equally interesting generalization of the problem by considering two laser beams of different polarization and of commensurate frequencies, such as the frequency ω for one of the two polarizations and frequency 3ω for the other polarization which looks to be a particularly promising generalization of our problem [21].

We assume that at moderate laser field intensities the interaction between the laser field and the atomic electron can be described by TDPT [20]. For the description of the dressing of the hydrogen ground state by the above field combination (1) we find it necessary to use *second-order perturbation theory*. Following the work of Florescu *et al* [22], the approximate solution for the ground state of an electron bound to a Coulomb potential in the presence of an electromagnetic field can be written in the form

$$|\Psi_1(t)\rangle = \mathrm{e}^{-\mathrm{i}E_1 t}\left[|\psi_{1\mathrm{s}}\rangle + |\psi_{1\mathrm{s}}^{(1)}\rangle + |\psi_{1\mathrm{s}}^{(2)}\rangle\right] \tag{4}$$

where $|\psi_{1\mathrm{s}}\rangle$ is the unperturbed ground state of the hydrogen atom, of energy E_1. The states $|\psi_{1\mathrm{s}}^{(1),(2)}\rangle$ denote the first- and second-order laser-field-dependent corrections, respectively. Using the results of the detailed investigations in [22, 23] these corrections can be expressed by means of the linear response

$$|\vec{w}_{1\mathrm{s}}(\Omega)\rangle = -G_{\mathrm{C}}(\Omega)\vec{P}|\psi_{1\mathrm{s}}\rangle \tag{5}$$

and by the quadratic response

$$|w_{ij,1\mathrm{s}}(\Omega', \Omega)\rangle = G_{\mathrm{C}}(\Omega')P_i G_{\mathrm{C}}(\Omega)P_j|\psi_{1\mathrm{s}}\rangle \tag{6}$$

where $G_{\mathrm{C}}(\Omega)$ is the Coulomb–Green function and $\vec{P}$ is the momentum operator of the bound electron. For our above field combination (1) there are five values of the argument of the Green functions necessary in order to write down the approximate solution (4), namely

$$\Omega^{\pm} = E_1 \pm \omega \qquad \Omega'^{\pm} = E_1 \pm 2\omega \qquad \widetilde{\Omega} = E_1. \tag{7}$$

The interaction between the field (1) and a scattered electron of kinetic energy E_k and momentum $\vec{k}$ can be described by the well known Gordon–Volkov solution

$$\chi_{\vec{k}}(\vec{r}, t) = \frac{1}{(2\pi)^{3/2}}\exp\left\{-\mathrm{i}E_k t + \mathrm{i}\vec{k}\cdot\vec{r} - \mathrm{i}\vec{k}\cdot\vec{\alpha}(t)\right\} \tag{8}$$

where $\vec{\alpha}(t)$ describes the classical oscillation of the electron in the electric field $\vec{\mathcal{E}}(t)$. The amplitude of this oscillation is given by $\alpha_0 = \sqrt{I}/\omega^2$. Using Graf's addition theorem of Bessel functions [24], the Fourier expansion of the Gordon–Volkov solution (8) leads to a series in terms of ordinary Bessel functions J_N of integer order N, namely

$$\begin{aligned} \mathrm{e}^{-\mathrm{i}\vec{k}\cdot\vec{\alpha}(t)} &= \exp\left\{-\mathrm{i}\alpha_0\vec{k}\cdot\vec{e}\sin\omega t - \mathrm{i}\mathcal{R}_k\sin(\omega t-\phi_k)\right\} \\ &= \sum_N J_N(\mathcal{Z}_k)\exp(-\mathrm{i}N\omega t)\exp(\mathrm{i}N\psi_k). \end{aligned} \tag{9}$$

Following the definitions of the arguments and phases given in Watson's book [24], we can write

$$\mathcal{Z}_k = \alpha_0|\vec{k}\cdot\vec{e} + \vec{k}\cdot\vec{\varepsilon}\,| \tag{10}$$

$$\mathcal{R}_k = \alpha_0|\vec{k}\cdot\vec{\varepsilon}\,| \tag{11}$$

and

$$\exp(\mathrm{i}\psi_k) = \frac{\vec{k}\cdot\vec{e} + \vec{k}\cdot\vec{\varepsilon}}{|\vec{k}\cdot\vec{e} + \vec{k}\cdot\vec{\varepsilon}|} \tag{12}$$

$$\exp(\mathrm{i}\phi_k) = \frac{\vec{k}\cdot\vec{\varepsilon}}{|\vec{k}\cdot\vec{\varepsilon}|} \tag{13}$$

respectively. In the above equations, the parameters $\mathcal{R}_k$ and ϕ_k refer to the CP field alone, while the other two parameters $\mathcal{Z}_k$ and ψ_k are related to our superposition of two fields in (1). Considering expressions (12) and (13), we recognize that a change of the helicity of the CP photons, corresponding to the replacement $\vec{\varepsilon} \to \vec{\varepsilon}^*$, will lead to a change in sign of the dynamical phases ϕ_k and ψ_k. Therefore, by searching for the signature of helicity in the angular distributions of the scattered electrons, it will be crucial to look for the presence of the dynamical phases in the expressions of the DCS.

As stated previously, we shall consider high energies of the scattered electrons. Hence the first Born approximation in terms of the scattering potential V will be sufficiently accurate. Neglecting exchange effects, the interaction potential will be given by $V(r, R) = -1/r + 1/|\vec{r}+\vec{R}|$, where $\vec{R}$ refers to the atomic coordinates. Then the scattering matrix element will be described by

$$S_{fi}^{\mathrm{B1}} = -\mathrm{i}\int_{-\infty}^{+\infty}\mathrm{d}t\,\langle\chi_{\vec{k}_f}(t)\Psi_1(t)|V|\chi_{\vec{k}_i}(t)\Psi_1(t)\rangle \tag{14}$$

where $\Psi_1(t)$ and $\chi_{\vec{k}_{i,f}}(t)$ are given by the dressed atomic state (4) and by the Gordon–Volkov states (8), respectively. $\vec{k}_{i(f)}$ represent the initial (final) momenta of the scattered electron.

The DCS for a scattering process in which N laser photons are involved can be written after Fourier decomposition of the S-matrix element (14) in the following standard form:

$$\frac{\mathrm{d}\sigma_N}{\mathrm{d}\Omega} = (2\pi)^4\frac{k_f(N)}{k_i}|T_N|^2. \tag{15}$$

The scattered electrons have the final energy $E_f = E_i + N\omega$, where N is the net number of photons exchanged between the colliding system and the radiation field (1). $N \geqslant 1$ refers to the absorption and $N \leqslant -1$ to the emission of laser quanta, while $N = 0$ corresponds to the elastic scattering process. In the foregoing equation (15), the nonlinear transition matrix elements T_N, obtained from the S-matrix element (14), have the following general structure:

$$T_N = \exp(\mathrm{i}N\psi_q)\left[T_N^{(0)} + T_N^{(1)} + T_N^{(2)}\right]. \tag{16}$$

where ψ_q is the dynamical phase defined in (12), referring here to the momentum transfer $\vec{q} = \vec{k}_i - \vec{k}_f$ of the scattered electron.

The first term in (16) of the expression for T_N,

$$T_N^{(0)} = -\frac{1}{4\pi^2} f_{\rm el}^{\rm B1} J_N(\mathcal{Z}_q) \tag{17}$$

would yield the well known Bunkin–Fedorov scattering formula [25] in which the dressing of the target atom is neglected and the atom gets described by a structureless potential. In this case the DCS reduces to the expression

$$\frac{{\rm d}\sigma_N}{{\rm d}\Omega} = \frac{k_f(N)}{k_i} |f_{\rm el}^{\rm B1}|^2 J_N^2(\mathcal{Z}_q) \tag{18}$$

and the ordinary Bessel function $J_N(\mathcal{Z}_q)$ contains all the radiation field dependences of the nonlinear scattering processes. $f_{\rm el}^{\rm B1}$ is the amplitude of elastic electron scattering in the first-order Born approximation. It reads in the case of a hydrogen atom as

$$f_{\rm el}^{\rm B1} = \frac{2\left(q^2+8\right)}{\left(q^2+4\right)^2}. \tag{19}$$

The other two terms in the transition matrix element (16) are related in our case to the dressing of the atomic ground state by the laser field (1). These terms were discussed in considerable detail in our previous work [18]. In particular, the second term $T_N^{(1)}$ of (16) refers to a first-order dressing of the atom in which case *one* of the N photons exchanged between the colliding system and the radiation field is interacting with the bound electron, while the third term $T_N^{(2)}$ describes second-order dressing and here *two* of the N photons exchanged during scattering interact with the atomic electron. These dressing terms in (16) for T_N can be written in the form

$$T_N^{(1)} = \frac{\alpha_0 \omega}{4\pi^2 q^2} \frac{|\vec{q}\cdot\vec{e} + \vec{q}\cdot\vec{\varepsilon}|}{q} \left[J_{N-1}(\mathcal{Z}_q) - J_{N+1}(\mathcal{Z}_q) \right] \mathcal{J}_{1,0,1}(\tau^+, \tau^-, q) \tag{20}$$

and

$$\begin{aligned} T_N^{(2)} = \frac{\alpha_0^2 \omega^2}{8\pi^2 q^2} \big\{ & J_{N-2}(\mathcal{Z}_q) \left[|\vec{q}\cdot\vec{e} + \vec{q}\cdot\vec{\varepsilon}|^2 q^{-2} \mathcal{T}_1 + (1 + 2\vec{e}\cdot\vec{\varepsilon})\, {\rm e}^{-2{\rm i}\psi_q} \mathcal{T}_2 \right] \\ & + J_{N+2}(\mathcal{Z}_q) \left[|\vec{q}\cdot\vec{e} + \vec{q}\cdot\vec{\varepsilon}|^2 q^{-2} \mathcal{T}_1 + \left(1 + 2\vec{e}\cdot\vec{\varepsilon}^*\right) {\rm e}^{2{\rm i}\psi_q} \mathcal{T}_2 \right] \\ & + J_N(\mathcal{Z}_q) \left[|\vec{q}\cdot\vec{e} + \vec{q}\cdot\vec{\varepsilon}|^2 q^{-2} \widetilde{\mathcal{T}}_1 + 2\left(1 + {\rm Re}\, \vec{\varepsilon}^*\cdot\vec{e}\right) \widetilde{\mathcal{T}}_2 \right] \big\}. \end{aligned} \tag{21}$$

The five radial integrals, denoted by $\mathcal{J}_{1,0,1}$, $\mathcal{T}_1$, $\mathcal{T}_2$, $\widetilde{\mathcal{T}}_1$ and $\widetilde{\mathcal{T}}_2$ in the foregoing equations (20) and (21), depend not only on the absolute value of the momentum transfer q, but also on the parameters of the Coulomb Green functions (7). The integral $\mathcal{J}_{1,0,1}$ is a function of the two parameters $\Omega^\pm$ by means of the relation $\tau^\pm = 1/\sqrt{-2\Omega^\pm}$, as specified in detail in [26], while the integrals $\mathcal{T}_1$, $\mathcal{T}_2$, $\widetilde{\mathcal{T}}_1$ and $\widetilde{\mathcal{T}}_2$ depend on four parameters since they are related to the second-order dressing of the target atom [18]. $\mathcal{T}_1$ and $\mathcal{T}_2$ in (21) are multiplied by the Bessel functions $J_{N-2}(\mathcal{Z}_q)$ if both laser photons are absorbed and they are multiplied by $J_{N+2}(\mathcal{Z}_q)$ if both photons are emitted by the atomic electron. Similarly, $\widetilde{\mathcal{T}}_1$ and $\widetilde{\mathcal{T}}_2$ that are multiplied by $J_N(\mathcal{Z}_q)$ belong to the case in which one photon is absorbed and another emitted by the bound electron. For the numerical evaluations performed in this paper, we used the analytic expressions for the above five radial integrals which are presented explicitly in [18, 27]. For the case of single-photon transitions equivalent expressions were published in [29–31] and for two-photon absorption or emission in [32].

The transition matrix elements $T_N^{(1)}$ and $T_N^{(2)}$ for first- and second-order laser dressing of the atom in (20) and (21) are written in a form which evidently permits one to analyse their dependence on the dynamical phase ψ_q. We recognize immediately that $T_N^{(0)}$ and $T_N^{(1)}$ do not depend on the helicity of the photon. On the other hand, $T_N^{(2)}$ exhibits such an explicit dependence on the photon helicity. This dependence is determined by the phase factors of $(1 + 2\vec{e} \cdot \vec{\varepsilon})\, \mathrm{e}^{-2\mathrm{i}\psi_q}$ and its complex conjugate by which $\mathcal{T}_2$ is multiplied in the first two terms of $T_N^{(2)}$ in (21).

In the introduction we have defined CDAD as the angular dependence of the difference between the DCS for a *left*- and a *right*-handed CP laser field. Hence, from our formulae (15)–(17) and (20) and (21), we obtain the following expression for the CDAD effect:

$$\Delta_{\mathrm{C}} = -\frac{k_f}{k_i}\frac{\alpha_0^2\omega^2}{q^2}\frac{1}{|\vec{q}\cdot\vec{e}+\vec{q}\cdot\varepsilon|^2}\left[J_{N-2}(\mathcal{Z}_q) - J_{N+2}(\mathcal{Z}_q)\right]\mathrm{Re}\left[\mathcal{P}^*\mathcal{T}_2\left(\mathcal{Q}-\mathcal{Q}^*\right)\right] \tag{22}$$

where the parameter

$$\mathcal{Q} = (\vec{e}+\vec{\varepsilon})^2\left(\vec{q}\cdot\vec{e}+\vec{q}\cdot\vec{\varepsilon}^{\,*}\right)^2 \tag{23}$$

contains all the helicity dependence of Δ_{C} since the other parameter

$$\begin{aligned}\mathcal{P}(q;\omega) = {} & f_{\mathrm{el}}^{\mathrm{B1}} J_N(\mathcal{Z}_q) - \alpha_0\omega\frac{|\vec{q}\cdot\vec{e}+\vec{\varepsilon}\cdot\vec{q}|}{q^3}\mathcal{J}_{1,0,1}\left[J_{N-1}(\mathcal{Z}_q) - J_{N+1}(\mathcal{Z}_q)\right] \\ & -\alpha_0^2\omega^2\frac{|\vec{q}\cdot\vec{e}+\vec{\varepsilon}\cdot\vec{q}|^2}{2q^4}\left\{\mathcal{T}_1\left[J_{N-2}(\mathcal{Z}_q) + J_{N+2}(\mathcal{Z}_q)\right] + \widetilde{\mathcal{T}}_1 J_N(\mathcal{Z}_q)\right\} \\ & -\alpha_0^2\omega^2\frac{|\vec{e}+\vec{\varepsilon}|^2}{2q^2}\widetilde{\mathcal{T}}_2 J_N(\mathcal{Z}_q)\end{aligned} \tag{24}$$

does not depend on it.

We can immediately convince ourselves that all three conditions (a)–(c), mentioned in the introduction, have to be fulfilled in order to obtain non-vanishing CDAD effects or $\Delta_{\mathrm{C}} \neq 0$. Indeed, we find:

(a) $\mathcal{Q} = 0$ in the absence of the linearly polarized laser field since then $\vec{\varepsilon}^{\,2} = 0$;
(b) $\mathcal{T}_2$ has its origin in the second-order laser-dressing of the target atom; and finally
(c) $\mathrm{Im}\,\mathcal{P} = 0$ and $\mathrm{Im}\,\mathcal{T}_2 = 0$ as soon as $2\omega < |E_1|$.

In fact, due to the structure of the expression for Δ_{C} in (22) we obtain $\Delta_{\mathrm{C}} = 0$ if $\mathcal{P}$ and $\mathcal{T}_2$ are real amplitudes since $\mathrm{Re}\,(\mathcal{Q} - \mathcal{Q}^*) = 0$. As was shown in [18, 26], the necessary conditions to obtain $\mathrm{Im}\,\mathcal{P} \neq 0$ and $\mathrm{Im}\,\mathcal{T}_2 \neq 0$ are to require $\omega > |E_1|$, or at least $2\omega > |E_1|$, in other words, to use laser frequencies such that one- or two-photon virtual transitions to continuum states are energetically allowed.

Moreover, our equation (22) shows that Δ_{C} is increasing with increasing laser frequency ω and that it is decreasing with the increase of the momentum transfer $\vec{q}$. Thus Δ_{C} is large at rather small scattering angles.

3. Weak-field limit of the transition matrix element

For small arguments of the Bessel functions $J_N(\mathcal{Z}_q)$, i.e. either for weak laser fields at any scattering angle or for moderate field intensities at small scattering angles, it is sufficient to retain the leading terms in T_N of (16) only [28]. Since we shall consider in our numerical examples moderate laser field intensities and small scattering angles, the approximation of the Bessel functions by their leading terms will be sufficient. We focus our attention on this angular domain since it is well known that target dressing is considerable there and thus the CDAD effects can be large as we have discussed before.

3.1. One-photon sidebands

Based on general considerations of angular momentum algebra, it has been argued that dichroic effects will not be encountered in one-photon transitions as long as they are treated in the lowest order of perturbation theory (LOPT) [16]. Indeed, retaining only the first order in the field dressing of the atom, we obtain from (16)

$$T_{\pm 1} = -\frac{\alpha_0}{8\pi^2 q^2}\,(\vec{q}\cdot\vec{e}+\vec{q}\cdot\vec{\varepsilon}\,)\left[f_{\rm el}^{\rm B1} \mp \frac{2\omega}{q^3}\mathcal{J}_{1,0,1}\right]. \tag{25}$$

However, the DCS are proportional to $|\vec{q}\cdot\vec{e}+\vec{q}\cdot\vec{\varepsilon}|^2$ and hence they are helicity independent in LOPT. For strong fields, however, we may obtain a non-vanishing $\Delta_{\rm C}$ due to higher-order corrections to the leading process, described by (25). These corrections involve at least three photons and a consistent treatment would imply higher-order target dressing.

3.2. Two-photon sidebands

We discuss now in some detail the case of two-photon transitions. In the case of absorption, $N = 2$, the corresponding transition matrix element reads

$$T_2 = \frac{\alpha_0^2}{8\pi^2 q^2}\big[\,(\vec{q}\cdot\vec{e}+\vec{q}\cdot\vec{\varepsilon}\,)^2\,\mathcal{A} + (1+2\vec{e}\cdot\vec{\varepsilon})\,\mathcal{B}\big] \tag{26}$$

where the invariant amplitudes $\mathcal{A}$ and $\mathcal{B}$ depend on q, the absolute value of the momentum transfer of the scattered electron, and on the photon frequency ω. They are given by

$$\mathcal{A}\,(q;\omega) = -\frac{q^2}{2^2}\left[f_{\rm el}^{\rm B1} - \frac{4\omega}{q^3}\mathcal{J}_{1,0,1} - \frac{4\omega^2}{q^4}\mathcal{T}_1\right] \tag{27}$$

$$\mathcal{B}\,(q;\omega) = \omega^2\mathcal{T}_2. \tag{28}$$

If we consider $N = -2$ (i.e. two-photon emission), then the complex conjugate of the CP polarization vector $\vec{\varepsilon}$ in (26) has to be used and the invariant amplitudes for the appropriate value of q have to be evaluated since $q = |\vec{k}_i - \vec{k}_f|$ is a function of N because $E_f = E_i + N\omega$.

The differential cross section formula that can be derived from the transition matrix element T_2 of (26) turns out to be

$$\frac{{\rm d}\sigma_2}{{\rm d}\Omega} = \alpha_0^4\frac{k_f}{k_i}\frac{1}{2^2q^4}\big\{|\vec{q}\cdot\vec{e}+\vec{q}\cdot\vec{\varepsilon}|^4|\mathcal{A}|^2 + |1+2\vec{e}\cdot\vec{\varepsilon}|^2|\mathcal{B}|^2$$
$$+2\,{\rm Re}\big[\,(\vec{q}\cdot\vec{e}+\vec{q}\cdot\vec{\varepsilon})^2\left(1+2\vec{e}\cdot\vec{\varepsilon}^{\,*}\right)\mathcal{A}\mathcal{B}^*\big]\big\}. \tag{29}$$

This formula is sensitive to the change of the helicity ξ, defined in (3), only if ${\rm Im}\,\mathcal{A} \neq 0$ and ${\rm Im}\,\mathcal{B} \neq 0$. As discussed previously, this happens if virtual transitions to continuum states are energetically allowed.

For two-photon absorption the expression of $\Delta_{\rm C}$ is obtained by keeping in (24) only terms of second order in the laser field strength and by putting $J_0 \simeq 1$ in (22). We thus obtain

$$\Delta_{\rm C} = \frac{k_f}{k_i}\frac{\alpha_0^4}{2q^4}\,{\rm Re}\big[\mathcal{A}^*\mathcal{B}\left(\mathcal{Q}-\mathcal{Q}^*\right)\big]. \tag{30}$$

We shall now discuss in some detail the angular dependence of the CDAD effects described by $\Delta_{\rm C}$, given in (30). Two cases turn out to be of particular interest.

First, we shall consider the angular behaviour of CDAD if we choose $\vec{e}\|\vec{e}_i$. Here the superposition of the linearly and circularly polarized radiation field can be easily described in

the dipole approximation by a vector of elliptic polarization of the form $\vec{\epsilon}$, given in (2). In this case we shall denote Δ_C by Δ_E and we find from (30)

$$\Delta_E = \frac{k_f}{k_i}\frac{\alpha_0^4}{q^4} q_i q_j \left(\sqrt{2}+1\right)^2 \mathrm{Im}(\mathcal{A}^*\mathcal{B}). \tag{31}$$

We have defined $q_{i;j}$ as the projections of the momentum transfer $\vec{q}$ on the axes of the vector $\vec{\varepsilon} = \left(\vec{e}_i + \mathrm{i}\vec{e}_j\right)/\sqrt{2}$ of circular polarization. The last expression, (31), leads to CDAD of the DCS plotted as a function of the azimuth φ for a fixed scattering angle θ. Nevertheless, Δ_E turns out to vanish if it becomes integrated over the azimuth φ. Our expression (31) can be readily compared with that of elliptic dichroism predicted for photoionization [16] (see the last formula on p 3763 of this reference).

In the second case, where we take $\vec{e}\|\vec{e}_j$, the CDAD formula reads

$$\Delta_C = -\frac{k_f}{k_i}\frac{\alpha_0^4}{q^4}\left[\frac{q_i^2}{\sqrt{2}} + q_i q_j - \frac{q_j^2}{\sqrt{2}}\right]\mathrm{Im}(\mathcal{A}^*\mathcal{B}). \tag{32}$$

If we choose in addition a scattering configuration in which the LP field is polarized along the direction of the ingoing electron momentum $\vec{k}_i$, i.e. $\vec{e}\|\vec{k}_i$, then in Δ_C the terms proportional to q_i^2 and q_j^2 will survive if the cross sections are integrated over the azimuthal plane. Therefore, we can conclude that by introducing into the problem a privileged direction, namely that of the initial momentum $\vec{k}_i$ of the scattered electron, we are led to an important additional asymmetry. Hence in this case the signature of the photon helicity ξ will be present not only in the angular distribution of the DCS in the azimuthal plane but also in the cross sections integrated over this plane.

At the end of this section we want to stress the importance of the general form of the T-matrix element (26). Indeed, a structure of the T-matrix element for two-photon interactions of the form

$$T_2 = (\vec{\varepsilon}_1 \cdot \vec{\varepsilon}_2)\, M + (\vec{\varepsilon}_1 \cdot \vec{v}'')(\vec{\varepsilon}_2 \cdot \vec{v}')N \tag{33}$$

was also encountered with CDAD in other laser-induced processes. In particular, we mention the processes of two-photon ionization [16, 19] and of two-photon detachment of H^- [33] but also the elastic scattering of x-rays by an atom in its ground state (if the radiation problem is treated beyond the dipole approximation [9]). Here, of course, the physical meaning of the vector quantities $\vec{v}'$ and $\vec{v}''$ will be specific to each of the processes considered. Thus in the expression (33) these vector quantities denote the versor of the photoelectron in photoionization and photodetachement or the photon momenta in x-ray scattering. In all of these cases CDAD is caused by the interference between the real and the imaginary parts of the amplitude (33) and two terms with different angular behaviour are needed in order to obtain such interference. Moreover, we should stress that in the examples mentioned previously, M and N were complex quantities. Our conditions imposed on the photon frequency ω, namely $\omega > |E_1|$ or $2\omega > |E_1|$, were designed to achieve the same purpose: to obtain a complex matrix element. Finally, we point out that in the case of photoionization or photodetachment of an unpolarized atomic system there will be no equivalent of the privileged direction which is given in our present process by the direction of propagation of the ingoing electron $\vec{k}_i$, as we have discussed before. Therefore, as a consequence of this lack of further asymmetry, the processes mentioned here will only show CDAD but there will be no integrated CD effects encountered.

4. Results and discussion

We shall present numerical results for CDAD and CD in laser-assisted electron–hydrogen scattering at high energies of the ingoing particle. We shall concentrate our analysis of the nonlinear bremsstrahlung processes on the two cases in which the number of photons exchanged between the scattering system and the laser field is $N = \pm 2$ since here the effects turn out to be large enough to be accessible to observation.

On the basis of the formalism developed in sections 2 and 3, we shall present the DCS $\mathrm{d}\sigma_N/\mathrm{d}\Omega$ evaluated from (15) for a fixed scattering angle θ as a function of the azimuth φ and, correspondingly, show the dichroism Δ_{C}, given by (22), in the azimuthal plane. As the initial energy of the scattered electrons we have taken $E_i = 100$ eV. As pointed out earlier, we have chosen a laser frequency that is close to an atomic resonance, namely $\omega = 10$ eV. For example, this frequency could be obtained as the first harmonic of a KrF laser source. We shall show numerical results for the moderate field intensity $I = 3.51 \times 10^{12}$ W cm^{-2}. The initial electron momentum $\vec{k}_i$ is taken to point along the z-axis, while the propagation direction of the CP laser beam will be orthogonal to this axis. In order to illustrate some of the main characteristic features of our problem, we decided to present our numerical results predominantly for the following two cases: (A) CD in the angular distribution only and (B) CD in the angular distribution and in the integrated cross section.

4.1. Circular dichroism in the angular distribution

Here we consider the vector of CP to be given by

$$\vec{\varepsilon} = \frac{\vec{e}_z + \mathrm{i}\vec{e}_x}{\sqrt{2}}. \tag{34}$$

It has helicity $\xi = 1$ and is known to describe left-handed (LH) circularly polarized laser light. Correspondingly, $\vec{\varepsilon}^*$ characterizes a radiation field of opposite helicity $\xi = -1$ and thus refers to right-handed (RH) circularly polarized light. With the above choice (34) of the CP vector the laser beam defines the y-axis. The linear polarization vector will be taken parallel to the direction of the initial electron momentum, $\vec{e} \| \vec{k}_i$. Therefore, the LP laser beam will propagate in the (x, y)-plane. In this configuration we then have $\vec{k}_i \| \vec{e} \| \mathrm{Re}\,(\vec{\varepsilon})$.

In figure 1(a) we have plotted for scattered electrons of final energy $E_f = E_i + 2\omega$ the φ dependence of the angular distribution of the DCS in the azimuthal plane at the fixed scattering angle $\theta = 10^\circ$. The data in this figure for LHCP are shown by a dotted curve and those for RHCP by a broken curve. We quite clearly see that the laser-assisted signals depend strongly on the helicity of the photon. In figure 1(b) we present the results for the CDAD effect. Since the argument $\mathcal{Z}_q$ of the Bessel functions is small, the relation (31) is a good approximation for describing the dichroic effects. In our present case, Δ_E is proportional to $\cos\varphi$ and we therefore added the signs '+' and '−' in the right and left lobes of panel (b) in order to indicate the signs of this angular dependence. Due to this φ dependence, Δ_E will yield a vanishing result if it is integrated over φ. Similar results and conclusions can be obtained for two-photon emission ($N = -2$), but the shapes of the angular distributions will be different since the final momentum k_f of the scattered electron depends on the sign of the emitted or absorbed laser photons.

Furthermore, we should like to discuss in some detail for $N = 2$ the angular behaviour of the three terms in the transition matrix element (16). Since at small scattering angles and moderate laser field intensities the argument $\mathcal{Z}_q$ of the Bessel functions is small, we shall use

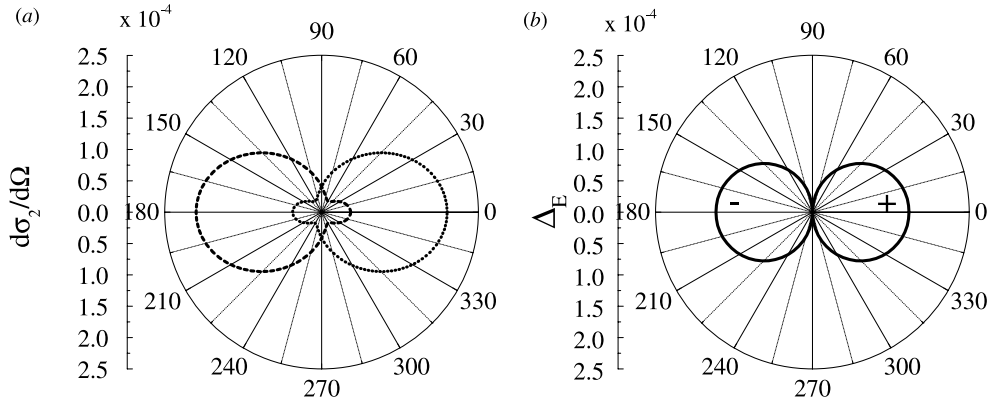

Figure 1. We present for the configuration (A) and for $N = 2$ the DCS $d\sigma_2/d\Omega$ as a function of the azimuthal angle φ at the scattering angle $\theta = 10^\circ$. The initial electron energy is $E_i = 100$ eV, the radiation frequency is $\omega = 10$ eV and the intensity is $I = 3.51 \times 10^{12}$ W cm^{-2}. The LP vector $\vec{e}$ points parallel to the initial momentum $\vec{k}_i$ of the ingoing electron while the CP vector $\vec{\varepsilon}$ lies in the (x, z)-plane and is chosen such that $\vec{k}_i \| \vec{e} \| \mathrm{Re}(\vec{\varepsilon})$. (*a*) Data for LHCP as a dotted curve and the data for RHCP as a broken curve. (*b*) CDAD effect as the difference between the dotted and broken data in (*a*) is clearly visible but we recognize that its integration over the azimuth φ will yield no net effect since the two lobes of equal magnitude have a different sign, as indicated.

for our discussion the approximate expression given in (26). When the laser dressing of the target atom becomes neglected, we find the angular distribution to be determined by $T_2^{(0)}$ of (17). This leads to the DCS

$$\frac{d\sigma_2}{d\Omega} \simeq \alpha_0^4 \frac{k_f}{k_i} \frac{1}{2^6} |\vec{q} \cdot (\vec{e} + \vec{\varepsilon})|^4 \left[f_{\mathrm{el}}^{\mathrm{B1}}(q) \right]^2 . \tag{35}$$

In figure 2(*a*) we show its φ-distribution for the same parameter values chosen initially. In this figure we denote by β the coefficient $(2\pi)^4 k_f / k_i$. This angular distribution turns out to be symmetric with respect to a reflection in the polarization plane (x, z) of the CP laser beam. It is, however, not the only symmetry axis in our figure because the replacement $\varphi = \pi/2 - \gamma \rightarrow \varphi' = \pi/2 + \gamma$ also yields a symmetry operation. Indeed, if we explicitly write down the expansion

$$|\vec{q} \cdot (\vec{e} + \vec{\varepsilon})|^4 = \sum_{j=0}^{2} c_j \cos^{2j} \varphi \tag{36}$$

where c_j are real coefficients which depend on k_i, k_f and θ, we realize that the above replacement shows a symmetry. Next we consider the contribution of the so-called mixed term, proportional to $|T_2^{(1)}|^2$ of (20). The corresponding angular distribution is plotted in figure 2(*b*). It has the same angular behaviour as the data in (*a*) but its values are four orders of magnitude larger since we have chosen the laser frequency $\omega = 10$ eV to match the atomic resonance 1s–2p and hence the contribution of $T_2^{(0)}$ is basically negligible. The final DCS, presented in (*d*), are then the result of the interference between the mixed $T_2^{(1)}$ and the atomic amplitude $T_2^{(2)}$, for which $|T_2^{(2)}|^2$ is shown in (*c*). The data for the latter have a different angular behaviour because of the φ-independent contributions determined by the integral $\mathcal{T}_2$.

We shall also briefly discuss a different scattering configuration in which the polarization plane of the CP field is orthogonal to the electron initial momentum $\vec{k}_i$. In this case both laser

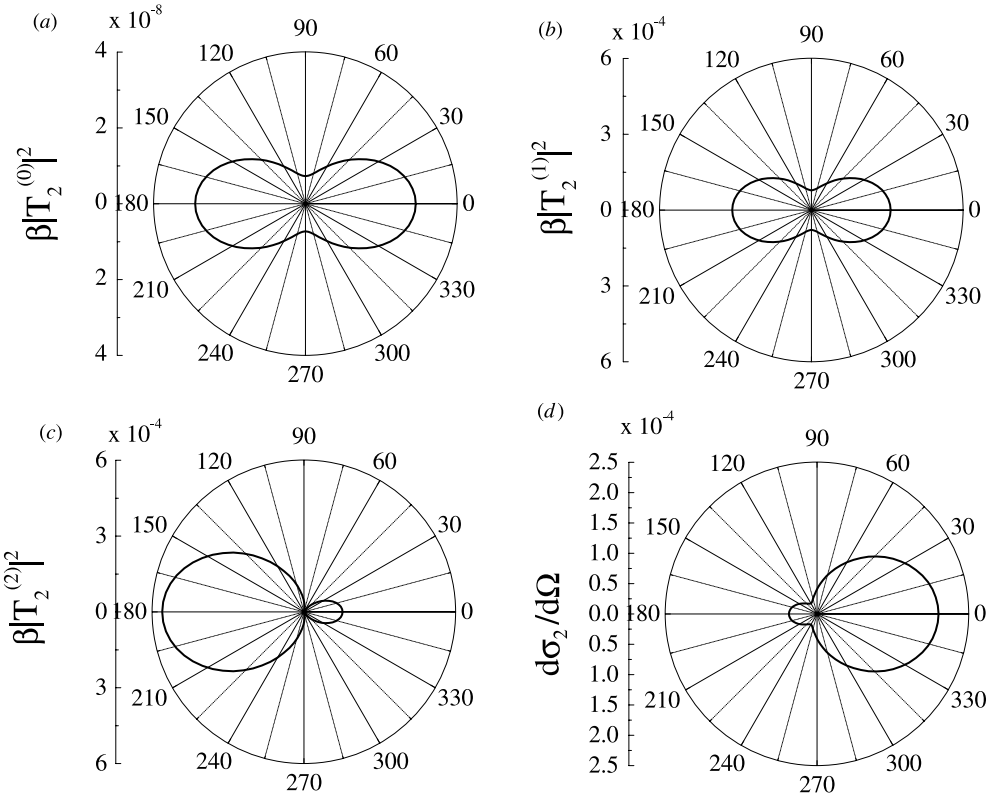

Figure 2. For the same configuration (A) and parameter values as in figure 1 we show for $N = 2$ in (a) the DCS as a function of the azimuthal angle φ as evaluated from the Bunkin–Fedorov approximation, determined by $T_2^{(0)}$. Here the abbreviation $\beta = (2\pi)^4 k_f/k_i$ has been introduced. In (b) we present the corresponding DCS data of the mixed contributions, coming from $T_2^{(1)}$. These data have the same angular dependence as those of (a) except that they are larger by four orders of magnitude. In (c) the atomic DCS contributions, given by $T_2^{(2)}$, are shown and in (d) we plotted the DCS $\mathrm{d}\sigma_2/\mathrm{d}\Omega$ evaluated from the total matrix element (16). These diagrams clearly show the contributions and interferences of the various terms leading to the final cross section data.

beams may propagate along the z-axis such that $\vec{\varepsilon} = \left(\vec{e}_x + \mathrm{i}\vec{e}_y\right)/\sqrt{2}$ and the LP field shall have its unit vector $\vec{e}$ parallel to the x-axis. The scattering results obtained in this configuration for two-photon absorption are shown in figure 3(a), using the same parameter values as in figure 1. As seen in figure 3(b), the dichroism Δ_E, which now is proportional to $\sin 2\varphi$, has a fourfold clover-leaf pattern. This same laser configuration was also considered in two-photon ionization [19] where the dichroic effects have the same φ dependence (see equations (11) and (14) of [19]). In figure 4 we have plotted the quantity

$$R(\varphi) = \frac{\Delta_E}{\mathrm{d}\sigma_2^{\mathrm{RH}}/\mathrm{d}\Omega + \mathrm{d}\sigma_2^{\mathrm{LH}}/\mathrm{d}\Omega} \tag{37}$$

using the Cartesian form of presenting the data. For comparison we refer to the typical results for $R(\varphi)$ obtained for two-photon ionization (the data of figure 4(b) of [19]).

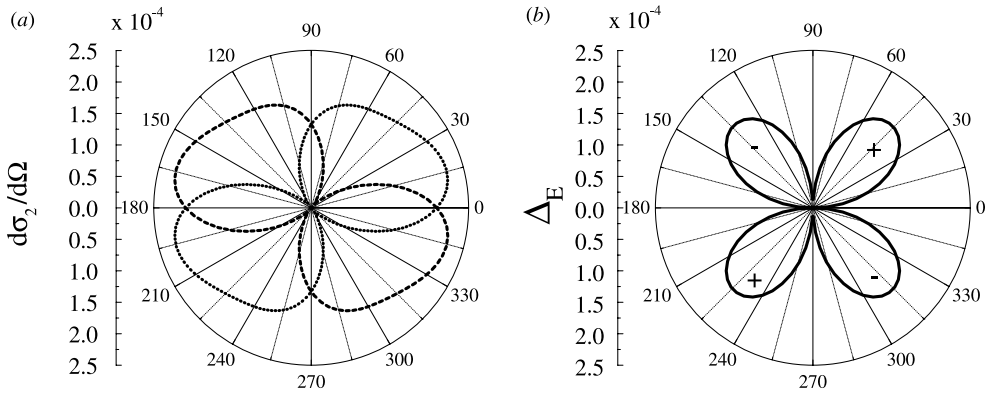

Figure 3. Here the polarization plane of the CP field is taken as orthogonal to the electron initial momentum $\vec{k}_i$. Both laser beams now propagate along the z-axis such that $\vec{\varepsilon} = \left(\vec{e}_x + \mathrm{i}\vec{e}_y\right)/\sqrt{2}$ and the LP field has $\vec{e}$ parallel to the x-axis. The scattering results for two-photon absorption ($N = 2$) are shown in (a) with a dotted curve for LHCP and a broken curve for RHCP, using the same parameter values as in figure 1. As seen in (b), the dichroism Δ_E, proportional to $\sin 2\varphi$, leads to a fourfold clover-leaf pattern. The present laser configuration was also considered in two-photon ionization [19].

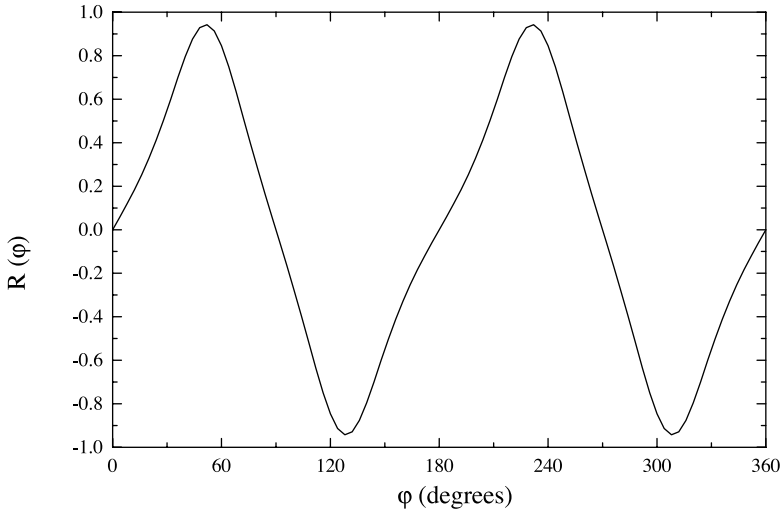

Figure 4. Using the same configuration as in figure 3, we plotted the quantity $R(\varphi)$, defined in (37), in the Cartesian form of presenting the data. These show, by comparison, the similarity with the typical results for $R(\varphi)$ obtained for two-photon ionization (see figure 4(b) of [19]).

4.2. Circular dichroism in the integrated cross section

We next discuss in some detail the angular behaviour of the DCS for the second configuration in which we choose the CP vector in the form

$$\vec{\varepsilon} = \frac{\vec{e}_y + \mathrm{i}\vec{e}_z}{\sqrt{2}} \tag{38}$$

so that we can now write $\vec{k}_i \| \vec{e} \|$ Im $(\vec{\varepsilon})$. Here the CP laser beam propagates along the x- axis, while the direction of propagation of the LP beam remains the same as before in the (x, y)-plane.

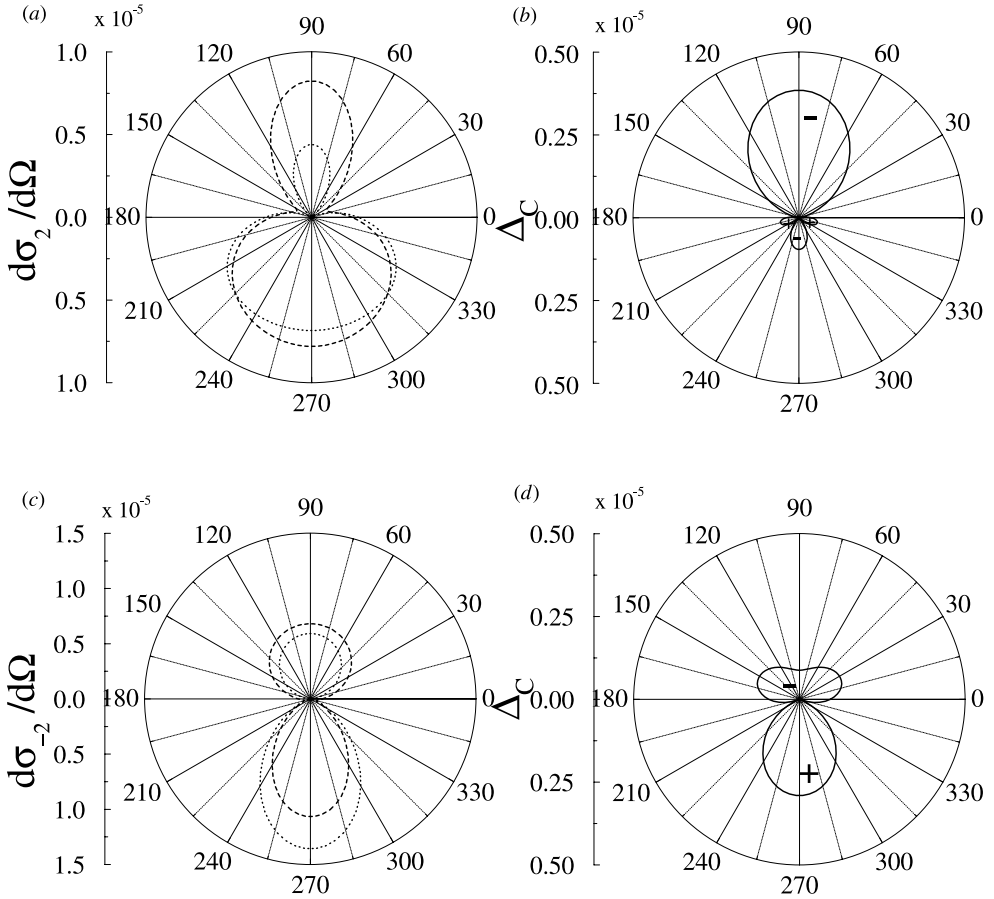

Figure 5. This figure presents for the other configuration (B), in which case $\vec{k}_i \| \vec{e} \| \mathrm{Im}\,(\vec{\varepsilon})$, but otherwise for the same parameter values as in figure 1, the φ dependence of the DCS and of Δ_C at fixed scattering angle $\theta = 10^\circ$ for $N = 2$ in (*a*) and (*b*) and for $N = -2$ in (*c*) and (*d*). In (*a*) a dotted curve is used for the DCS of LHCP and a broken curve for those of RHCP. (*b*) The corresponding result for Δ_C as given by (32). As is clearly visible, for the present field configuration Δ_C does not vanish if integrated over φ. Since the final momentum $\vec{k}_f$ of the scattered electron depends on N, the shape of the angular distribution of the DCS and the φ dependence of Δ_C are different for $N = -2$ as seen in (*c*) and (*d*) if compared with the data for $N = 2$.

In our figure 5 we show the φ dependence of the DCS (15) at fixed scattering angle $\theta = 10^\circ$ for two-photon absorption in (*a*) and for two-photon emission in (*c*). In (*a*) we have used dotted curves for LHCP and broken curves for RHCP. In (*b*) we present the corresponding result for Δ_C, as given by (22). For the present choice of the laser field configuration we have from (32)

$$q_j^2 - \sqrt{2} q_i q_j - q_i^2 = (k_i - k_f \cos\theta)^2 + \sqrt{2}(k_i - k_f \cos\theta) k_f \sin\theta \sin\varphi - k_f^2 \sin^2\theta \sin^2\varphi \tag{39}$$

and we can immediately recognize that, on account of this angular dependence, Δ_C will not vanish if it becomes integrated over the azimuth φ. Since, as we have pointed out before, the final momentum k_f of the scattered electron depends on N (its value and sign), the shape of

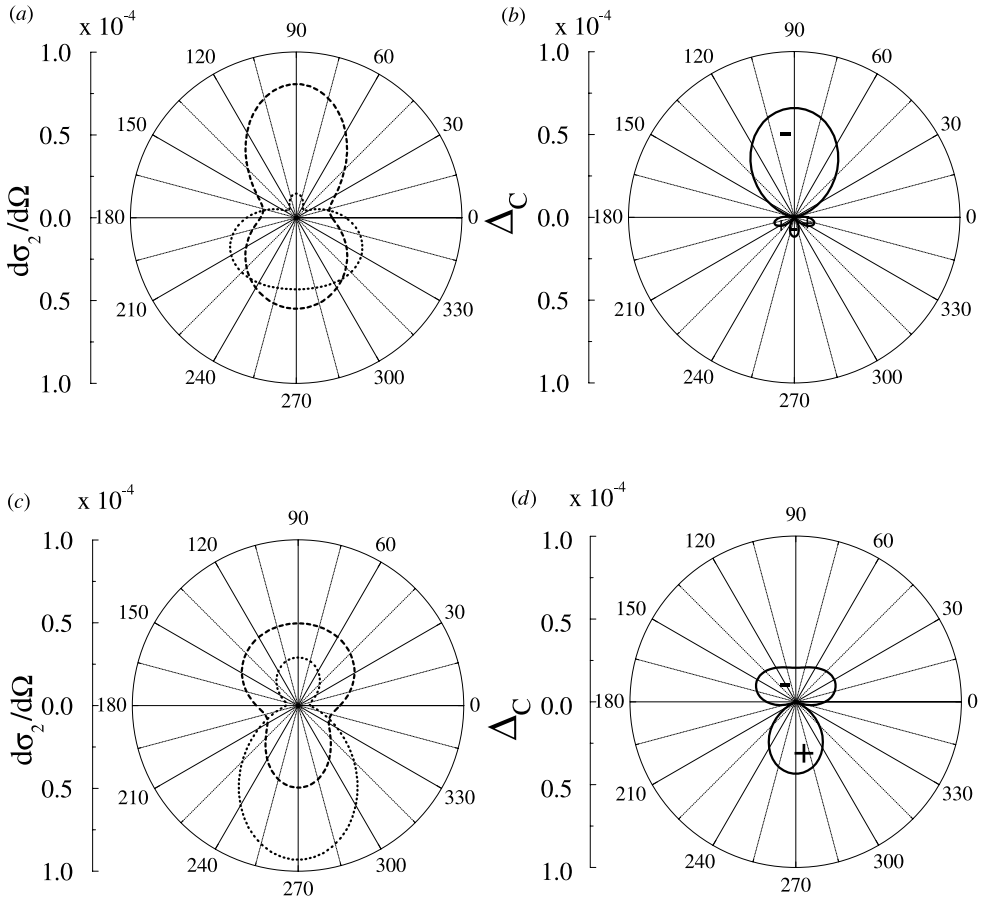

Figure 6. This figure demonstrates the strong θ dependence of the DCS and of CDAD. In our case it cannot be factorized as in the problem of two-photon ionization [19]. We present the φ dependence of the DCS and of Δ_C for the same parameter values as in figure 5, but for $\theta = 20^\circ$. Panels (*a*) and (*b*) are for $N = 2$ and (*c*) and (*d*) for $N = -2$, where (*a*) and (*c*) show the DCS and (*b*) and (*d*) present Δ_C. Note, in particular, in (*b*) for $N = 2$ the comparatively simple shape of Δ_C. As it turns out, $\theta = 20^\circ$ is close to the kinematic minimum for absorption [32] given by $\cos\theta = k_i/k_f$. At this scattering angle the φ dependence of Δ_C is then close to $-\sin^2\varphi$.

the angular distribution of the DCS and the φ dependence of Δ_C are different for two-photon emission in (*c*) and (*d*), if compared with the results for absorption.

It is interesting to note that in free–free transitions there is a strong θ dependence of the DCS and of CDAD, as well. Here this θ dependence cannot be factorized as in the case of two-photon ionization, as seen, for example, in equations (11) and (14) of the work of Taieb *et al* [19]. We therefore present in figure 6 the φ dependence of the DCS and of Δ_C for the same parameter values as in figure 5, but for $\theta = 20^\circ$. Panels (*a*) and (*b*) are for $N = 2$ and (*c*) and (*d*) for $N = -2$. For $N = 2$ we note the comparatively simple shape of Δ_C in panel (*b*). Indeed, $\theta = 20^\circ$ is close to the kinematical minimum that exists for absorption [32]. It is determined by the condition $\cos\theta = k_i/k_f$. Considering (39), we see that at this scattering angle the φ dependence of Δ_C is close to $-\sin^2\varphi$.

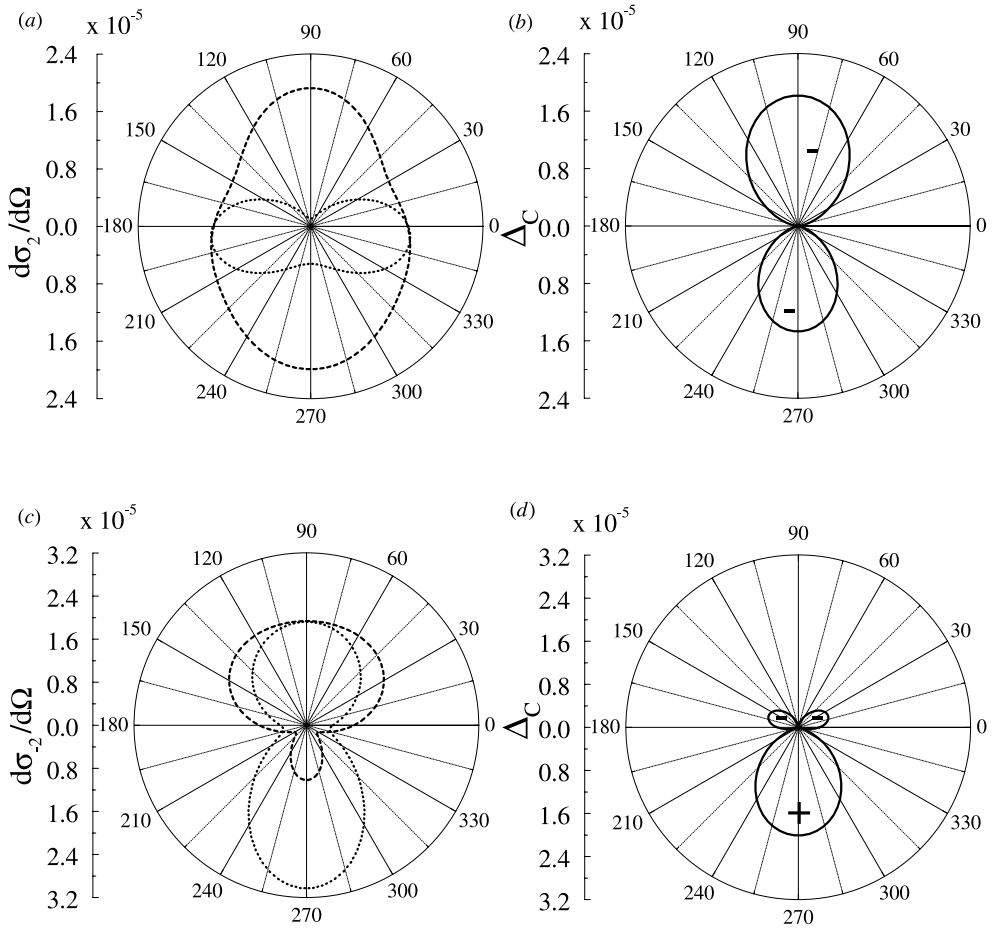

Figure 7. The scattering probabilities decrease with increasing laser frequency ω. Hence a frequency close to an atomic resonance was chosen in figures 1–6 to enhance the signals. Dichroism is, however, not a resonance effect. We demonstrate this by showing for the configuration (B) the angular distribution of the DCS and the dichroic effects for $\omega = 9$ eV where (*a*) and (*b*) show the data for $N = 2$ and (*c*) and (*d*) for $N = -2$. The other parameter values are the same as in figure 1. Even here, considerably off-resonance, Δ_C is between 30% and 50% of the DCS.

Since the scattering probabilities decrease with increasing laser frequency ω we preferred to choose a frequency that is close to an atomic resonance and to thus find an enhancement of the signals. Dichroic effects are, however, by no means resonance effects. In order to illustrate this point we show in figure 7 the angular distribution and the dichroic effects for $\omega = 9$ eV. The other parameters are the same as in figure 5. Even in this case Δ_C amounts to between 30% and 50% of the DCS.

Our data in the above figures show that the maximum amount of dichroism that can be achieved in our problem can reach a value of up to $\frac{2}{3}$ of the laser-assisted scattering signal. This result is therefore comparable in magnitude to, or even larger than, the size of the corresponding effect predicted in x-ray scattering [9] or in two-photon ionization in a bichromatic field [19]. We should also point out that, similar to what was predicted in the case of x-ray scattering, the effect of dichroism increases if the radiation frequency increases. This, in fact, is so since

at high energy of the scattered electrons the dichroism in our problem of free–free transitions originates in the second-order target dressing and these dressing effects increase with the frequency of the laser photons. Since we know that target dressing is particularly significant for rather small scattering angle, we have to expect that the effect of dichroism will be large in this angular domain, and not near $\theta = \pi/2$ as in the case of x-ray scattering or of two-photon photoionization.

Finally, we can ask ourselves whether the above two choices of the configuration of the two laser beams and of their polarizations are unique for observing the CDAD effects. Of course, they are not. We also considered two other cases in which $\vec{e} \| \operatorname{Im} \vec{\varepsilon}$. One such different configuration, namely choosing the vector of circular polarization $\vec{\varepsilon} = (\vec{e}_z + \mathrm{i}\vec{e}_x)/\sqrt{2}$ and the vector of linear polarization $\vec{e}$ parallel to the x-axis, turns out to be appropriate for observing CDAD and CD if in addition the initial electron momentum $\vec{k}_i$ points along the z-axis. In this case q_z is φ-independent and the term q_z^2 in (32) survives when integration is performed in the azimuthal plane. For another configuration in which $\vec{\varepsilon} = \left(\vec{e}_x + \mathrm{i}\vec{e}_y\right)/\sqrt{2}$ and the LP vector is taken parallel to the y-axis we can only observe CDAD if the initial electron momentum $\vec{k}_i$ continues to point along the z-axis and is therefore orthogonal to the plane of circular polarization. One can immediately check that here, according to (32), the CDAD effects vanish when they become integrated over φ since we find that $\Delta_C \sim k_f^2 \sin^2\theta\left(\cos^2\varphi + \sqrt{2}\sin\varphi\cos\varphi - \sin^2\varphi\right)$.

5. Summary and conclusions

To summarize, we have investigated the scattering of high-energy electrons by hydrogen atoms in the presence of a laser field of moderate power but high frequency. The laser field was composed of two components of equal frequency and intensity. One of the components was chosen to be circularly polarized, while the other one had linear polarization. The two laser beams were permitted to have different directions of propagation. As we were able to demonstrate, in this kind of scattering configuration circular dichroism in two-photon transitions can be predicted under the following conditions: the scattering of the high-energy electrons is treated in the first-order Born approximation, the laser dressing of the atomic target is carried out in second-order time-dependent perturbation theory and transitions between the atomic bound states and continuum states are energetically allowed. We showed that CDAD is closely related to the interference of different quantum paths involving photons with different states of polarization. If the linearly polarized laser field is turned off, the CDAD effects disappear, as we have shown in great detail in our previous work [18]. At high scattering energies, CDAD turns out to be a consequence of the second-order target dressing by the two laser fields and therefore higher laser frequencies should be involved in order to match the condition of transitions between bound and continuum states. In order to overcome the problem that the scattering signals decrease with increasing laser frequency ω, we had to choose a frequency close to an atomic resonance.

We conclude from our considerations in this paper that at high energies of the scattered particles circular dichroism in laser-assisted electron–atom scattering is a second-order field-assisted effect. It is not unlikely that similar effects will show up, if higher-order terms of the Born series are taken into account to describe the scattering process, since it is well known that in this case the scattering matrix elements become complex quantities. The work of Mittleman [12] and of Manakov *et al* [6] appears to support this conclusion.

Finally, we stress the role of the two asymmetries which we have introduced into the configuration of our scattering process in order to obtain helicity-dependent nonlinear signals. One asymmetry was introduced by adding to the CP laser beam the LP component, which was sufficient to obtain circular dichroism in the angular distributions. Introducing as a second asymmetry the direction of propagation of the ingoing electrons, i.e. taking $\vec{k}_i \| \vec{e} \| \mathrm{Im}\,(\vec{\varepsilon})$, we were then led to a CD effect that does not vanish on integrating the DCS over the azimuthal plane. The absence of such a privileged direction, like $\vec{k}_i$, in other processes, such as for example photoionization and photodetachment, explains why only CDAD is encountered in those latter cases. The analysis of the structure of the matrix elements of two-photon transitions ($N = \pm 2$) permitted us to write down the general form of a scattering amplitude that leads to CDAD and to thus understanding the physical reasons for the choice of configuration necessary to obtain circular dichroism in the angular distributions as well as in the integrated cross sections.

Acknowledgments

The authors should like to thank Professor Anthony F Starace for a most valuable detailed and clarifying discussion on various aspects of circular dichroism. One of us (AC) also wishes to acknowledge information by Professor Pierre Agostini concerning experiments on circular dichroism presently performed by his group. This work has been supported by the Jubilee Foundation of the Austrian National Bank under project number 6211 and by a special research project for 2000/1 of the Austrian Ministry of Education, Science and Culture.

References

[1] Cotton A 1896 *Ann. Chim. Phys.* **8** 360
[2] Born M 1981 *Optik* (Berlin: Springer)
[3] Born M and Wolf E 1991 *Principles of Optics* (Oxford: Pergamon)
[4] Cherepkov N A 1992 *Physics of Electronic and Atomic Collisions* ed W R McGillivray, I E McCarthy and M C Standage (Bristol: Hilger)
[5] Cherepkov N A, Kuznetsov A A and Verbitskii V A 1995 *J. Phys. B: At. Mol. Opt. Phys.* **28** 1221
[6] Manakov N L, Marmo S I and Volovich V V 1995 *Phys. Lett.* A **204** 48
[7] Kheifets A, Bray I, Soejima K, Danjo A, Okubo K and Yagishita A 1999 *J. Phys. B: At. Mol. Opt. Phys.* **32** L501
[8] Heinäsmäki S 1999 *J. Phys. B: At. Mol. Opt. Phys.* **32** 4321
[9] Manakov N L, Meremianin A V, Carney J P J and Pratt R H 2000 *Phys. Rev.* A **61** 032711
[10] Balashov V V and Golokhov E I 1999 *Phys. Lett.* A **257** 70
[11] Bashkansky M, Bucksbaum P H and Schumacher D W 1988 *Phys. Rev. Lett.* **60** 2458
[12] Mittleman M H 1993 *J. Phys. B: At. Mol. Opt. Phys.* **26** 2709
[13] Du N Y, Starace A F and Cherepkov N A 1993 *Phys. Rev.* A **48** 2413
[14] Manakov N L 1996 *Super-Intense Laser–Atom Physics* ed H Muller and M V Fedorov (Dordrecht: Kluwer)
[15] Cionga A and Buică G 1998 *Laser Phys.* **8** 164
[16] Manakov N L, Maquet A, Marmo S I, Véniard V and Ferrante G 1999 *J. Phys. B: At. Mol. Opt. Phys.* **32** 3747
[17] Rapoport L A and Kornev A S 1999 *Zh. Eksp. Teor. Fiz.* **116** 1241 (Engl. transl. 1999 *Sov. Phys.–JETP* **89** 664) See also Rapoport L A and Kornev A S 2000 *J. Phys. B: At. Mol. Opt. Phys.* **33** 87
[18] Cionga A, Ehlotzky F and Zloh G 2000 *Phys. Rev.* A **61** 063417
[19] Taïeb R, Véniard V, Maquet A, Manakov N L and Marmo S I 2000 *Phys. Rev.* A **62** 013402
[20] Byron F W Jr and Joachain C J 1984 *J. Phys. B: At. Mol. Phys.* **17** L295
[21] Cionga A, Ehlotzky F and Zloh G unpublished
[22] Florescu V, Halasz A and Marinescu M 1993 *Phys. Rev.* A **47** 394
[23] Florescu V and Marian T 1986 *Phys. Rev.* A **34** 4641
[24] Watson G N 1962 *Theory of Bessel Functions* 2nd edn (Cambridge: Cambridge University Press) p 359
[25] Bunkin F V and Fedorov M V 1965 *Zh. Eksp. Theor. Fiz.* **49** 1215 (Engl. transl. 1966 *Sov. Phys.–JETP* **22** 884)
[26] Cionga A and Florescu V 1992 *Phys. Rev.* A **45** 5282

[27] Cionga A and Zloh G unpublished
[28] Cionga A and Zloh G 1999 *Laser Phys.* **9** 69
[29] Dubois A, Maquet A and Jetzke S 1986 *Phys. Rev.* A **34** 1888
[30] Dubois A and Maquet A 1989 *Phys. Rev.* A **40** 4288
[31] Francken P and Joachain C J 1987 *Phys. Rev.* A **35** 1590
[32] Kracke G, Briggs J S, Dubois A, Maquet A and Véniard V 1994 *J. Phys. B: At. Mol. Opt. Phys.* **27** 3241
[33] Frolov M V, Manakov N L, Marmo S I and Starace A F 2000 *ICAP 2000 (Florence, 4–9 June)*